

Spiraling and Folding: The Topological View*

Jan Kynčl[†] Marcus Schaefer[‡] Eric Sedgwick[§] Daniel Štefankovič[¶]

June 17, 2022

Abstract

For every n , we construct two curves in the plane that intersect at least n times and do not form spirals. The construction is in three stages: we first exhibit closed curves on the torus that do not form double spirals, then arcs on the torus that do not form spirals, and finally pairs of planar arcs that do not form spirals. These curves provide a counterexample to a proof of Pach and Tóth concerning string graphs.

1 Introduction

In a surface, draw a pair of simple curves with a large number of intersections. Must the drawing contain any particular substructures? And if so, can these structures be used to simplify the drawing? Affirmative answers to these questions can be used to bound the complexity of certain types of drawings, such as those yielding string graphs. A *string graph* is the intersection graph of curves in the plane or some other surface. The recognition problem for string graphs is an old problem [2, 5, 14], [1, Research problem 1] that was solved in the planar case [13] by establishing an exponential bound on the complexity of such drawings.¹ Pach and Tóth [8] also claimed a solution to the string graph problem, but as we will see in Section 4.2 their proof contains a serious gap. What is so tricky about this problem?

Starting with a drawing of a pair of simple curves, one can increase the number of intersections by taking a part of one curve and dragging it over another curve. This creates a *bigon*, a disk region bounded by exactly one subarc of each curve, whose interior is disjoint from the curves; see Figure 1. Of course, there is an obvious simplification of

*An earlier version of this paper appeared in the proceedings of the 19th Canadian Conference on Computational Geometry [12].

[†]Charles University, Prague, Czech Republic; kyncl@kam.mff.cuni.cz. Supported by project 22-19073S of the Czech Science Foundation (GAČR) and by Charles University project UNCE/SCI/004.

[‡]DePaul University, Chicago, IL 60604, USA; mschaefer@cdm.depaul.edu

[§]DePaul University, Chicago, IL 60604, USA; esedgwick@cdm.depaul.edu

[¶]University of Rochester, Rochester, NY 14627, USA; stefanko@cs.rochester.edu

¹The problem is decidable on arbitrary surfaces, as shown in [11].

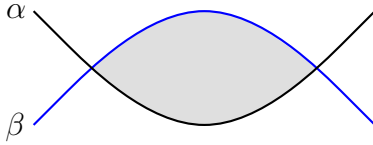


Figure 1: A bigon formed by α and β .

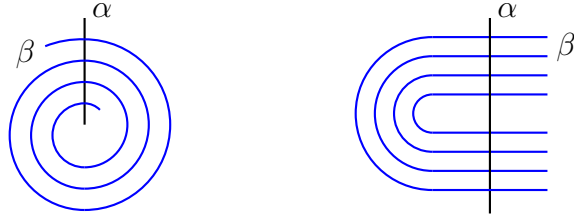


Figure 2: Left: A spiral formed by α and β . Right: A fold formed by α and β . The vertical arc is a part of the curve α , all the other arcs are parts of the curve β .

such a drawing. We call a drawing *reduced* if it contains no bigon. It is not hard to create a reduced drawing with many intersections, so the question arises: do such drawings contain some other type of structure?

One candidate for such a structure is a *fold*, pictured on the right in Figure 2. The drawing of the fold can be made into a reduced drawing by adding an endpoint to the center bigon or by altering the topology of the underlying surface in the bigon. Kratochvíl and Matoušek [7] use folds to create string graphs requiring $\Omega(2^n)$ intersections in any realization.

The focus in the current paper is a third structure, the *spiral*, pictured on the left in Figure 2. Spirals can be used to simplify certain drawings. For example, Pach and Tóth [8] demonstrate that spirals can be used to reduce the complexity of string graphs in the plane. However, in this and an earlier companion paper [10], we exhibit drawings with an arbitrary number of intersections and no spirals. The companion paper shows that certain drawings in the torus are spiral-free by analyzing intersection words. Here we use topological techniques to construct spiral-free drawings both in the torus and in the plane. All the drawings are reduced and the torus drawings are also fold-free. Thus, eliminating spirals and folds is not sufficient to bound the complexity of drawings in the torus (or surfaces of higher genus). And, as we show in Section 4.2, spiral-free planar drawings are a counterexample to Pach and Tóth's claim that wide folds imply the existence of a spiral (or a bigon) [8].

In the next section, we define the basic concepts including spirals and train tracks. In Section 3, we use train tracks to describe spiral-free drawings in the torus. Then, in Section 4, we show how to use the spiral-free torus drawings to construct spiral-free drawings in the plane.

2 Curves in Surfaces

In this section we introduce basic terminology for curves in surfaces, show how they can be represented using train tracks and develop basic facts on spirals.

2.1 Curves

We refer the reader to [3, 4, 16] for a basic reference on the topology of surfaces. Here we consider *surfaces* to be compact and orientable. We allow surfaces to have boundary components (which can be obtained by puncturing a closed surface). A *disk* is a surface that is homeomorphic to the closed unit disk, that is, the closure of the region bounded by the unit circle in the plane. An *annulus* is a surface that is homeomorphic to the closure of the region bounded by two concentric circles in the plane.

A *simple arc* in a surface F is an image of an injective continuous map from the closed unit interval $[0, 1]$ to F . A *simple closed curve* or a *simple loop* in a surface F is an image of an injective continuous map from the unit circle to F . A *simple curve* is a simple arc or a simple closed curve. If α is a simple arc, we denote by $\partial\alpha$ the two-element set of its endpoints. If α is a simple closed curve, then $\partial\alpha = \emptyset$. In other words, a simple curve in F is a connected 1-manifold embedded in F (with no self-intersections). We will refer to simple curves shortly as *curves*, and we use the term *multicurve* to refer to the union of finitely many pairwise disjoint simple curves. A simple closed curve α is *essential* in a compact surface F if α does not bound a disk in F , and α is not homotopic² to any boundary component of F .

A curve (or multicurve) α in a surface F with boundary is *properly embedded* in F if it is simple and it meets the boundary of F exactly in its endpoints (if any); that is, $\alpha \cap \partial F = \partial\alpha$.

An *isotopy* of a curve is a continuous deformation (homotopy) of that curve that, at each point in time, is a proper embedding of the curve. For properly embedded simple arcs we also insist that the isotopy fixes the endpoints. Two curves are *isotopic* if there is an isotopy between them.

In drawings of more than one curve, we assume that the curves are in general position in the sense that they do not touch or overlap; if two curves intersect, they have to do so transversely. Let $|\alpha \cap \beta|$ denote the number of intersection points between curves α and β .

2.2 Bigons

Let D be a disk and α and β be arcs that are properly embedded in D . The arcs α and β form a *bigon* B in D if they intersect precisely twice in D . In this case, the *bigon* B will be the closed disk region bounded by subarcs of α and β . We say that a pair of curves α and β form a *bigon* in a surface F if there is a disk $D \subset F$ such that subarcs of α and β form a bigon in D .

²Two curves are *homotopic* if they can be continuously deformed into each other.

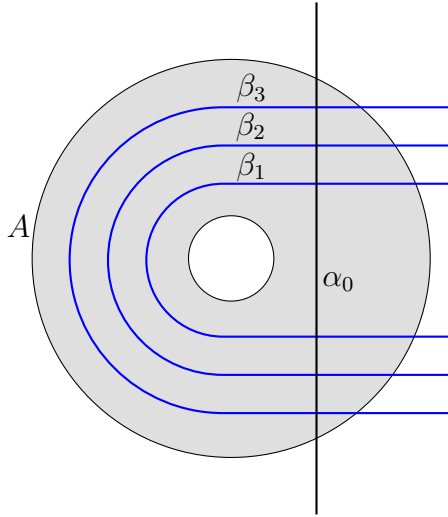


Figure 3: A fold of width 3 formed by α and β in A .

If α and β do not bound a bigon, we will say that their intersection is *reduced*. We say that a drawing consisting of a set of curves is *reduced* if all pairs of curves in the drawing have reduced intersection.

2.3 Folds

Let A be an annulus and α, β be two curves. Let $\alpha_0, \beta_1, \beta_2, \dots, \beta_k$ be arcs properly embedded in A with distinct endpoints on the outer boundary curve of A , such that $\alpha \cap A = \alpha_0$ and $\beta \cap A = \bigcup_{i=1}^k \beta_i$. The arcs α and β form a *fold of width k* in A if they have reduced intersection (no bigons) in A and every β_i intersects α_0 in exactly two points in A . See Figure 3. If a boundary curve of the annulus defining a fold bounds a disk in the total surface F , then this forces a bigon, so the drawing is not reduced.

2.4 Spirals

Let A be an annulus and β and γ be *spanning arcs* for A , that is, arcs properly embedded in A and with endpoints in opposite boundary curves of A . The arcs β and γ form a *d -spiral* in A if they have distinct endpoints, have reduced intersection (no bigons) in A , and intersect in $d + 2$ points in A . See Figure 4. The dashed lines indicate the possibility that β and γ are subarcs of larger curves, and other subarcs of the larger curves may also be present in the annulus A . If $d \geq 1$, we say that β and γ form a *spiral* in A .

A pair of curves β and γ in a surface F form a *d -spiral in F with respect to an annulus $A \subset F$* if subarcs of β and γ form a d -spiral in A . Again, if $d \geq 1$, we say that β and γ form a *spiral in F (with respect to A)*.

Note that β and γ forming a spiral in F is equivalent to the existence of a “singular”

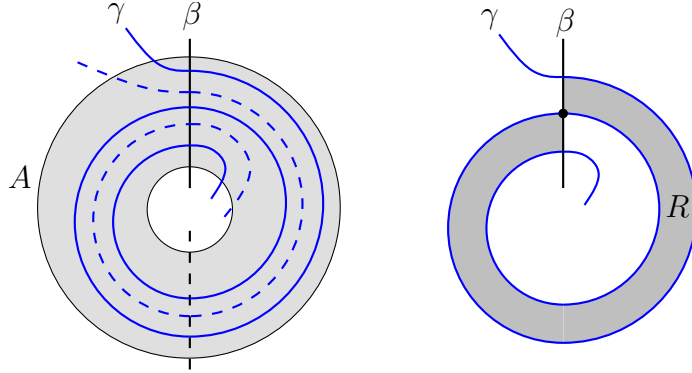


Figure 4: β and γ form a 1-spiral. The dashed lines indicate that other subarcs may be present.

rectangle $R \subset F$, a region formed by one subarc of β and one subarc of γ , whose interior is homeomorphic to an open disc, but its boundary path meets itself in exactly one point; see Figure 4.

Lemma 1. *Suppose that β, β', γ and γ' are spanning arcs for an annulus A with pairwise reduced intersection. If $\beta \cap \beta' = \gamma \cap \gamma' = \emptyset$, then $||\beta \cap \gamma| - |\beta \cap \gamma'|| \leq 1$ and $||\beta \cap \gamma| - |\beta' \cap \gamma'|| \leq 2$.*

The lemma uses $|\cdot|$ in two different meanings: applied to sets it is the cardinality of the set, applied to numbers it is the absolute value.

Proof. Since γ and γ' are disjoint they cut the annulus A into two rectangles, R_1 and R_2 as illustrated in Figure 5. The arc β has one endpoint on the top of a rectangle, say R_1 , and another endpoint on the bottom of a rectangle, either R_1 or R_2 . Since β has reduced intersection with both γ and γ' , there are no bigons in either rectangle. Aside from the two arcs meeting the top and bottom of the rectangles, every other subarc of β in a rectangle is horizontal, joining opposite sides. If the top and bottom endpoints of β are both in R_1 , then all subarcs of β in R_2 are horizontal, implying that $|\beta \cap \gamma| = |\beta \cap \gamma'|$. Otherwise, the top endpoint of β is in R_1 and the bottom endpoint in R_2 . In this case, we have $||\beta \cap \gamma| - |\beta \cap \gamma'|| = 1$.

The second inequality follows by two applications of the first: $||\beta \cap \gamma| - |\beta' \cap \gamma'|| = ||\beta \cap \gamma| - |\beta \cap \gamma'| + |\beta \cap \gamma'| - |\beta' \cap \gamma'|| \leq ||\beta \cap \gamma| - |\beta \cap \gamma'| + ||\beta \cap \gamma'| - |\beta' \cap \gamma'|| \leq 2$. \square

Lemma 2. *Suppose that the curves β and γ have reduced intersection and form a d -spiral in a surface F with respect to an annulus A . Let α be one of the two boundary curves of A . Let $k = |\beta \cap \alpha|$ and $l = |\gamma \cap \alpha|$. Then*

$$|\beta \cap \gamma| \geq dkl + k + l.$$

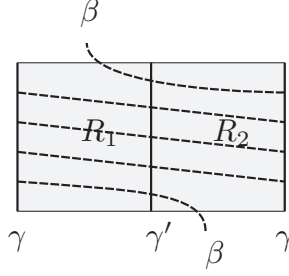


Figure 5: β passing through R_1 and R_2

Proof. The curve β meets the annulus A in at least k spanning arcs, β_1, \dots, β_k . Similarly, γ meets A in at least l spanning arcs, $\gamma_1, \dots, \gamma_l$.

By the definition of spiral, some pair (β_1, γ_1) , has $d+2$ intersections in A . By Lemma 1, pairs of the form (β_i, γ_1) where $i \neq 1$ and (β_1, γ_j) where $j \neq 1$ each have at least $d+1$ intersections in A . Also, by Lemma 1, pairs of the form (β_i, γ_j) with $i \neq 1, j \neq 1$ have at least d intersections in A . The total number of intersections between β and γ in A is therefore at least

$$(d+2) + (d+1)(k-1+l-1) + d(k-1)(l-1) = dkl + k + l.$$

This serves as lower bound on $|\beta \cap \gamma|$, the total number of intersections of β and γ . \square

Lemma 2 establishes a lower bound on $|\beta \cap \gamma|$ but there could be many more intersections for two reasons: First, β and γ may meet elsewhere in the surface F , the lemma only counts intersections in A . Second, the lemma allows for *slippage*: While the subarcs of β and γ that form the d -spiral intersect $d+2$ times, others pairs of subarcs from β and γ may slip and can have as few as d intersections in A (see Lemma 1). For example, if you take 2 close parallel copies of each of the arcs that form a 1-spiral, there will be $12 = 4 \cdot 3$ intersections in A , while the lemma only guarantees $8 = 1 \cdot 2 \cdot 2 + 2 + 2$. The lower bound of 8 can be realized by letting the second arcs slip, see the left side of Figure 4.

Lemma 3. *Let β and γ be properly embedded multicurves that have reduced intersection in F . Let β_1, β_2 be subarcs of β and γ_1, γ_2 subarcs of γ so that for some $d_1, d_2 \geq 1$,*

- β_1 and γ_1 form a d_1 -spiral in F with respect to an annulus A_1 , and
- β_2 and γ_2 form a d_2 -spiral in F with respect to an annulus A_2 .

If the defining annuli A_1 and A_2 are disjoint in F but have boundary curves that are isotopic in F then β and γ form a $(d_1 + d_2)$ -spiral in F .

Proof. Since the boundaries of the two annuli are parallel, there is another annulus between A_1 and A_2 . In this situation, we have concentric spirals such as those pictured in Figure 6. A priori, the spirals could wind in opposite directions. It will be a consequence of the

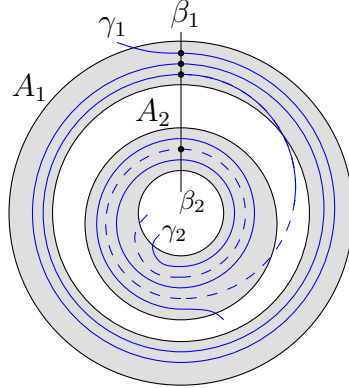


Figure 6: Concentric 1-spirals imply a 2-spiral. In this figure β_1 connects to β_2 in A but γ_1 does not connect to γ_2 in A .

assumptions and prove that this actually does not occur, see Remark 4. Regardless, call the union of all three annuli A .

Let β'_1 and γ'_1 be the arcs obtained by extending β_1 and γ_1 along β and γ until they exit A . (The arcs cannot close up because β_1 and γ_1 have an endpoint on the boundary of A , so they must exit as there are no endpoints in the interior of A .) Then β'_1 and γ'_1 must be spanning arcs for A : Suppose, for contradiction, that one of them, say β'_1 , does not span A and instead has both endpoints on the same boundary component of A ; see Figure 7. Then β'_1 bounds a disk (a bigon) B in A with that boundary component of A . But, β'_1 forms a d_1 -spiral ($d_1 \geq 1$) with γ'_1 in $A_1 \subset A$, which means that γ'_1 meets β'_1 at least 3 times in A . Inside B at most two of these intersections can be connected to the boundary A by a subarc of γ'_1 . It follows that there must be another subarc of $\gamma'_1 \cap B$ that has both endpoints on β'_1 . This forms a smaller bigon between β'_1 and γ'_1 inside B and contradicts the assumption that β and γ have reduced intersection. Thus β'_1 and (by a symmetric argument) γ'_1 are spanning arcs.

By assumption β'_1 and γ'_1 have at least $d_1 + 2$ intersections in A_1 . Since they span A they also pass through A_2 , where they either subsume or remain disjoint from the subarcs β_2 and γ_2 , respectively. In the worst case neither is subsumed, but Lemma 1 still guarantees that β'_1 and γ'_1 have at least $d_2 + 2 - 2 = d_2$ additional intersection in A_2 . Therefore β'_1 and γ'_1 have at least $d_1 + d_2 + 2$ intersections in A , so the total curves β and γ form a $(d_1 + d_2)$ -spiral in A (and F). \square

Remark 4. The reader may wonder about the case when the concentric spirals wind in opposite directions, one clockwise and one counter-clockwise. In fact, this does not occur because the intersection is assumed to be reduced. In the above proof, if the spirals wound in opposite directions, then a bigon would be formed whose corners were the last intersection between β'_1 and γ'_1 in A_1 and the first additional intersection between β'_1 and γ'_1 in A_2 (they have opposite algebraic sign).

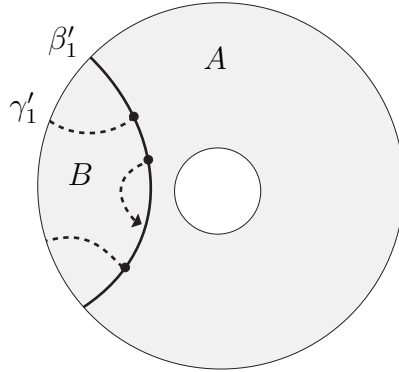


Figure 7: If β'_1 does not span A , then the intersection between β'_1 and γ'_1 is not reduced.

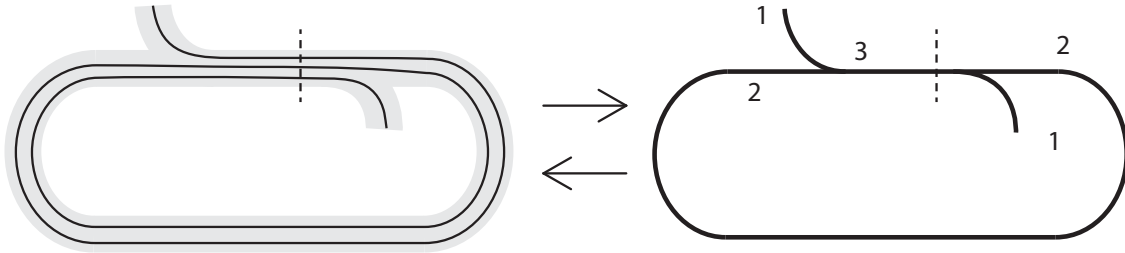


Figure 8: A multicurve and the corresponding weighted train track. The dashed arc is a basis arc for the branch with weight 3. That basis arc and the multicurve form a 1-spiral in a neighborhood of the track.

2.5 Train Tracks

Train tracks give us a shorthand for drawing complicated multicurves on a surface. The basic idea is captured in Figure 8. In a complicated multicurve it can be hard to differentiate individual subarcs that take a similar path. A weighted train track embraces their similarity by combining these subarcs and noting their count.

We now give a more formal definition, for a reference, see [9]. A *train track* is a graph T that is smoothly embedded in a surface F . All vertices must have degree 1 or 3. The vertices of degree one are called *terminals*, the vertices of degree three are called *switches*, and the edges are called *branches*. The embedding into F must be smooth in the sense that: a) the interior of each branch/edge is a smooth curve, and b) at each switch, two of the branch ends meeting the switch are smooth extensions of the third. A *basis curve* for a branch is a simple curve (either an arc or closed curve) in F that meets the train track transversely in a single point on that branch.

We specify an embedded multicurve in an arbitrarily small neighborhood of the track T by assigning a *weight* w_i , a non-negative integer, to each branch. The *weight vector* \vec{w} will

denote the collection of weights for each branch. The weighted track $\{T|\vec{w}\}$ determines a unique (up to isotopy) multicurve in the neighborhood of the track, where the weights indicate the number of times the multicurve travels along each branch. We ensure that the multicurve respects the tangency conditions at the switches by requiring that the weights at each switch of T satisfy a *matching equation*: the sum of the weights of the branches entering a switch is equal to the weight of the branch exiting. For example, in the track in Figure 12, the two switches yield the same matching equation, $p = q + r$. Note that we overload the notation, using a variable (such as p, q, r) to both label a branch as well as to indicate the weight of a multicurve on that branch. We also adopt the convention that a branch meeting a terminal has weight 1, which means it represents the endpoint of an arc in the resulting multicurve. We say that T carries a multicurve $\beta \subset F$ if there is a set of weights on T that induces β and satisfies the matching equations.

We say that a weighted train track $\{T|\vec{w}\}$ contains a d -spiral if some component of the multicurve determined by the weights forms a d -spiral in a neighborhood of the track with a basis arc for a branch of T . In Figure 8 the weighted train track contains a 1-spiral because the curve specified by the weights forms a 1-spiral with a basis arc that crosses the branch labeled 3.

3 Avoiding Spirals on the Torus

In Section 3.2 we construct a spiral-free drawing of two (reduced) curves on the torus with an arbitrary number of intersection points. As a preparatory step, Section 3.1 shows how to build a pair of closed curves avoiding 2-spirals.

3.1 Fibonacci Curves: 2-Spiral-Free Curves on the Torus

Our goal is to build for any given m a pair of closed curves on the torus that have at least m intersections but that do not form a d -spiral for $d \geq 2$.

Fortunately, it is easy to represent essential closed curves on the torus, see for example Stillwell [16, Sections 6.2.2, 6.4.2, 6.4.3]. First, one chooses a (non-unique) *basis*, which is a pair of curves, μ and λ that intersect once. We can think of the longitude, λ , as the curve that goes the “long” way around the torus once and the meridian, μ , as a curve that goes once around the “short” way. (This is a highly prejudicial view, but one that won’t lead us astray). Then any closed multicurve on the torus, γ , can be represented by an ordered pair of integers, measuring the number of times the curve wraps longitudinally and the number of times the curve wraps meridionally.

Now, we classify intersection patterns between two closed curves in the torus, see Figure 9. Let α and β be oriented essential simple closed curves on the torus with reduced intersection consisting of p points. Choose one of the intersection points and label it as the origin 0. On each curve, start at the origin and travel along the curve in the direction of its orientation. This induces a parameterization of each curve by the interval $[0, p)$, where the intersection points are $\{\alpha(0) = 0, \alpha(1), \dots, \alpha(p - 1)\}$ along α and

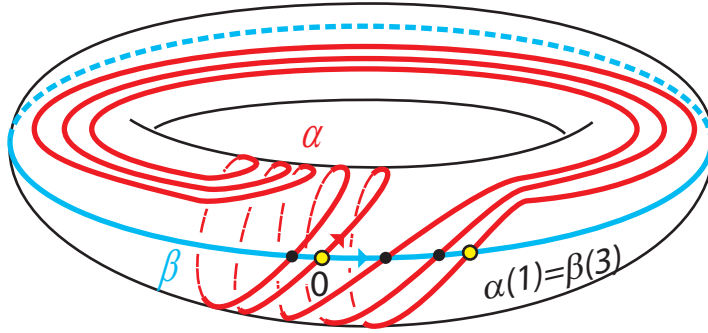


Figure 9: Computing the shift, $q = 3$. The curves α and β intersect with pattern $(5, 3)$.

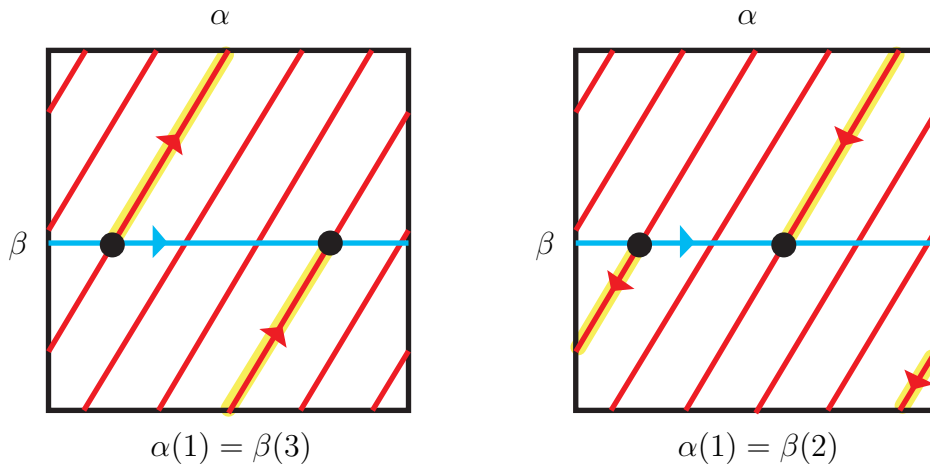


Figure 10: Reversing α (or β) changes the intersection pattern from (p, q) to $(p, p - q)$. The highlight traces the curve to compute the shift.

$\{\beta(0) = 0, \beta(1), \dots, \beta(p - 1)\}$ along β . We write $\alpha([a, b])$ for the subcurve of α between points $\alpha(a)$ and $\alpha(b)$ (and similarly for β). We say that the *shift* of α with respect to β is the value q for which $\beta(q) = \alpha(1)$. It is well known that, for curves with reduced intersection, the intersection pattern is transitive; that is, there is an orientation-preserving homeomorphism of the torus that preserves α and β and takes any intersection point to any other. It follows that the shift q is independent of the choice of the origin 0 .

If α meets β in p points with shift q then p and q are relatively prime and $0 \leq q < p$, and we will say that α intersects β with *pattern* (p, q) . Also note that reversing the direction of α moves the intersection point q units in the opposite direction along β , so the resulting shift will be $p - q$.

We say that a d -spiral between oriented curves α and β is *positive* if the $d + 2$ intersections that define the spiral are encountered in the same order when traveling positively along both α and β .

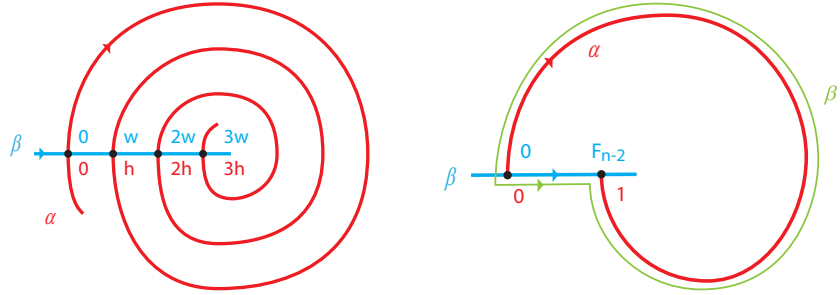


Figure 11: A 2-spiral, forming β' .

Remark 5. It is not hard to see that if α and β are essential simple closed curves on the torus whose reduced intersection consists of 3 or more points, then α and β form a 1-spiral in the torus, since for any intersection pattern (p, q) we have $\min(q, p - q) < p/2$.

Let $F_0 = 0, F_1 = 1, F_2 = 1, \dots$ be the sequence of Fibonacci numbers. The goal of this section is to prove Theorem 7 which says that a pair of simple closed curves on the torus with intersection pattern (F_n, F_{n-1}) do not form a 2-spiral. The next lemma rules out the possibility of a *negative* 2-spiral for, as noted above, a *negative* 2-spiral between curves with pattern (F_n, F_{n-1}) is equivalent to a *positive* 2-spiral between curves with pattern $(F_n, F_n - F_{n-1}) = (F_n, F_{n-2})$. The proof is by induction. After showing that there are no “wide” 2-spirals, we show that a positive 2-spiral between curves with pattern (F_n, F_{n-2}) implies a positive 2-spiral with pattern (F_{n-2}, F_{n-4}) .

Lemma 6. *Let α and β be simple closed curves on the torus with reduced intersection. If α intersects β with pattern (F_n, F_{n-2}) , $n \geq 2$, then α and β form no positive 2-spiral.*

Proof. We induct on n . The result is trivially true for $n \leq 4$ because α and β have at most $F_4 = 3$ intersections, not enough to form a 2-spiral which requires at least 4 distinct intersections.

Suppose that $n \geq 4$ and that α and β form a positive 2-spiral. See Figure 11. The complement of the spiral has two rectangular regions. Each rectangle has subarcs of α as its left and right sides and subarcs of β as its top and bottom sides. As the curves have reduced intersection, any other arc (not drawn) that crosses one side of a rectangle, say the left, must continue through the rectangle and cross the opposite, say right, side. So parallel sides of the rectangles have the same number of intersections. Thus we can define the *width* and the *height* of the spiral as the positive integers w and h , respectively, such that the four intersections that define the spiral occur at positions $\beta(0) = \alpha(0) = 0, \beta(w) = \alpha(h), \beta(2w) = \alpha(2h)$ and $\beta(3w) = \alpha(3h)$.

First, a 2-spiral cannot be too wide, specifically we show that $F_{n-2} > 3w$: Suppose to the contrary that $F_{n-2} \leq 3w$. Since $\alpha(1) = \beta(F_{n-2})$, it must be that this point occurs somewhere in the interval $\beta([0, 3w])$. And as it is the first intersection along α it follows that $h = 1$ and $w = F_{n-2}$. But then $3F_{n-2} = 3w < F_n = 2F_{n-2} + F_{n-3}$, a contradiction.

Since $F_{n-2} > 3w$, the arcs $\alpha([0, 1])$ and $\beta([0, F_{n-2}])$ meet only in their endpoints and thus their union $\beta' = \alpha([0, 1]) \cup \beta([0, F_{n-2}])$ is a simple closed curve. Moreover if we slide β' slightly in the negative direction with respect to β , see Figure 11, it is a closed curve that meets α in F_{n-2} points. Every time α crosses β' at one of these points it crosses in the same direction (same algebraic sign). It follows both that β' is essential and that α and β' have reduced intersection.

Now compute the shift of α with respect to β' : All intersection points between α and β' lie on the subarc $\beta([0, F_{n-2} - 1])$ of β' . So when we travel along α , starting from $\alpha(0) = \beta'(0)$, we encounter intersections with β . But only those in the interval $\beta([0, F_{n-2} - 1])$ are also intersections with β' . So when does α return to the interval $\beta([0, F_{n-2} - 1])$? The first intersection of α with β is the point $\alpha(1) = \beta(F_{n-2})$. But this is just beyond the interval $\beta([0, F_{n-2} - 1])$ so it is not an intersection with β' . The second is at $\alpha(2) = \beta(2F_{n-2})$. But, $2F_{n-2} < F_n$, so this is still not an intersection with β' . Finally, the third intersection is at the point $\alpha(3) = \beta(3F_{n-2})$. As we should only consider the latter coordinate modulo F_n , we have

$$3F_{n-2} \pmod{F_n} = 3F_{n-2} - F_n = 3F_{n-2} - (2F_{n-2} + F_{n-3}) = F_{n-4}.$$

So the shift of α with respect to β' is F_{n-4} and α and β' intersect with pattern (F_{n-2}, F_{n-4}) . Moreover, α and β' , because they have subarcs $\alpha([0, 3h])$ and $\beta([0, 3w])$ which form a positive 2-spiral, also form a positive 2-spiral. This contradicts the inductive hypothesis. \square

Theorem 7. *Let α and β be simple closed curves on the torus with reduced intersection. If α intersects β with pattern (F_n, F_{n-1}) , $n \geq 2$, then α and β form no 2-spiral.*

Proof. First observe that by reorienting one of the curves we obtain curves intersecting with pattern $(F_n, F_n - F_{n-2}) = (F_n, F_{n-2})$, which form no positive 2-spiral by Lemma 6, see also Figure 10. This implies that α and β form no negative 2-spiral.

Suppose that α and β form a positive 2-spiral. We proceed similarly as in proof of Lemma 6: As before, the base cases $n = 2, 3$ hold because the curves do not have enough intersections. For $n \geq 4$ we conclude that $F_{n-1} \geq 3w$ because $\beta(F_{n-1}) = \alpha(1)$. Then we observe α and $\beta' = \beta([0, F_{n-1}]) \cup \alpha([0, 1])$ have F_{n-1} intersections. The shift is computed by noting that $F_{n-1} < F_n < 2F_{n-1}$ so the curve “rolls over” after two original shifts, that is, the shift of α with respect to β' is

$$2F_{n-1} - F_n = F_{n-1} - F_{n-2} = F_{n-3}.$$

Thus α and β' intersect with pattern (F_{n-1}, F_{n-3}) and form a positive 2-spiral. This contradicts Lemma 6. \square

3.2 Spiral-Free Curves on the Torus

Figure 12 shows two views of the same weighted train track T_0 on a torus. In the left hand picture opposite sides of the square are identified in order to form a torus. Let μ be the

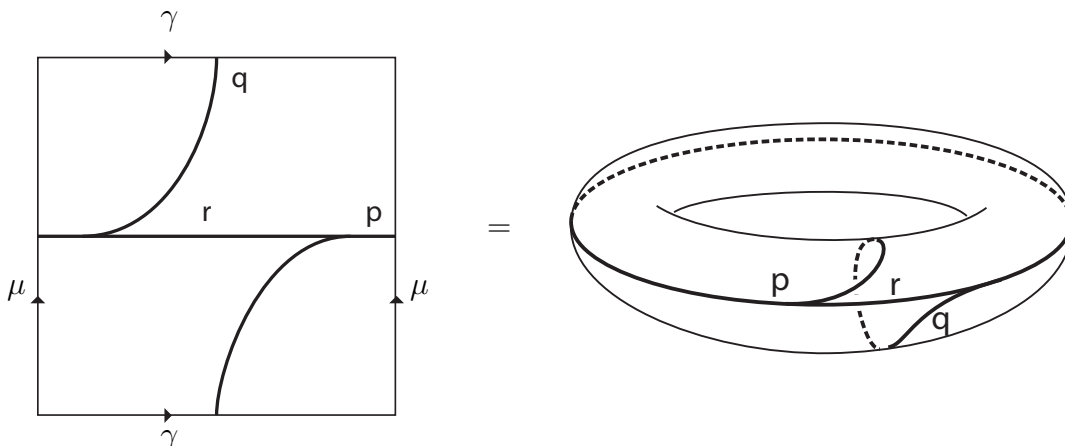


Figure 12: Two views of the train track T_0 on a torus. The torus is formed by identifying opposite sides of the rectangle together, that is, left to right and top to bottom. The weighted train track $\{T_0|p = F_n, q = F_{n-1}, r = F_{n-2}\}$ contains no d -spiral for $d \geq 2$.

curve formed by identifying the left and right sides of the rectangle and oriented upwards, and λ the curve formed by identifying the top and bottom of the rectangle and oriented from left to right. Then μ and λ intersect once and thus form a (homology) basis for the torus. Moreover, they also serve as basis curves for two branches of T_0 . The train track T_0 carries all closed multicurves on the torus whose coordinates (p, q) satisfy $p \geq 0, q \geq 0$; these coordinates are exactly the weights of the corresponding branches of the train track. (Recall that when considering un-oriented curves, we may always assume $m \geq 0$.)

Corollary 8. *The weighted train track $\{T_0|p = F_n, q = F_{n-1}, r = F_{n-2}\}$ contains no d -spiral for $d \geq 2$.*

Proof. Let γ_n be the (connected) multicurve that lives in a neighborhood of T_0 and that is prescribed by the weights $p = F_n, q = F_{n-1}, r = F_{n-2}$. Recall that we say that the weighted train track contains a 2-spiral if γ_n forms a spiral with a basis arc of one of the branches, which are labeled p, q and r . In fact, if the 2-spiral uses the basis arc of q or r , then we can extend it to a 2-spiral that uses the basis arc of the branch labeled p : Suppose, for instance, that the spiral is formed with a basis arc of the, say, r branch. Then extend that arc across the q branch, and slide it across the switch where the p branch meets the q and r branches. This yields a basis arc for the p branch that defines a 2-spiral for the weighted track.

Thus if T_0 contains a 2-spiral, then γ_n and μ form a 2-spiral contradicting Theorem 7, because γ_n intersects μ with pattern (F_n, F_{n-1}) , the shift arising from the F_{n-1} arcs that travel along the branch labeled q . \square

Consider the train track T_1 pictured in Figure 13(a). We identify opposite edges of the square so this train track is embedded in the torus. In this section we will demonstrate that $\{T_1|p = P = F_n - 1, q = Q = F_{n-1} - 1, r = R = F_{n-2} - 1, \text{ terminals have weight } 1\}$ is spiral-free. Note that the weights of some branches are not specified, but each such

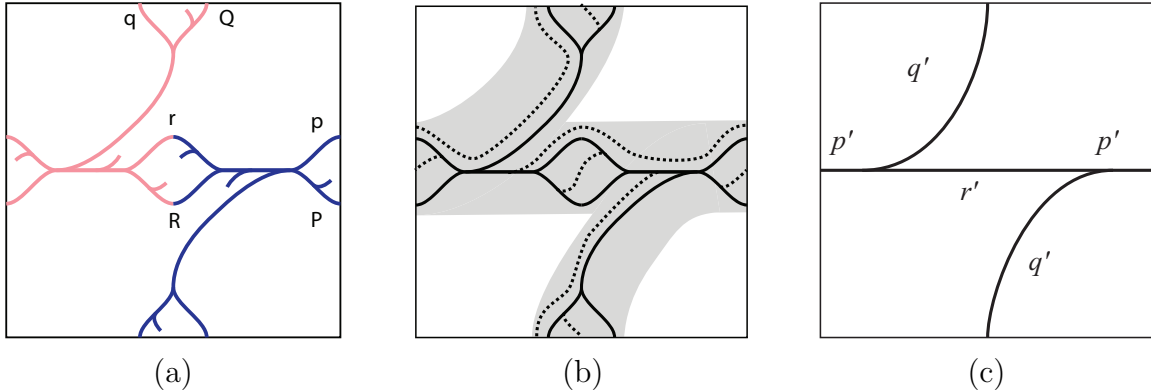


Figure 13: a) The train track T_1 . The weighted train track $\{T_1 | p = P = F_n - 1, q = Q = F_{n-1} - 1, r = R = F_{n-2} - 1, \text{ terminals have weight } 1\}$ has no 1-spirals. b) Extending curves in T_1 to closed curves in T_0 . c) The train track T_0 .

unspecified weight is uniquely determined as the the sum of the weights on the incoming branches.

The most interesting property of the track T_1 is that it is fixed under the self-homeomorphism of the torus, call it π , that is obtained by rotating the square about its center through the angle π . Note that π is an involution, that is, it is its own inverse. Moreover, π is orientation-preserving and acts on the branches of T_1 by changing the case of each branch, exchanging branches with lower case labels with branches with upper case labels. The only fixed points of the involution π as it acts on the torus are: the center of the square; the corners of the square, all of which are identified to a single point; and the midpoint of each edge of the square (opposite edges are identified). Since the track T_1 avoids all of these points, the restriction of π to T_1 is fixed-point-free. Fix a small neighborhood of T_1 , $N(T_1)$, that also avoids the fixed points, and is fixed setwise by π , so that $\pi : N(T_1) \rightarrow N(T_1)$ is a self-homeomorphism. We can also choose short basis arcs for each branch of T_1 that are pairwise disjoint and such that their union is preserved by π setwise. We highlight the following fact, which is established by the choice of $N(T_1)$.

Lemma 9. *The involution π has no fixed point in $N(T_1)$.*

If any simple arc drawn in $N(T_1)$ is preserved setwise by π , then π would have a fixed point in that arc, hence in $N(T_1)$. Lemma 9 then implies the following.

Corollary 10. *The involution π preserves no simple arc carried by T_1 .*

Note that the train track T_1 can be naturally embedded inside a neighborhood of the train track T_0 , see Figure 13(b). Using this embedding we define an extension of any multicurve γ carried by T_1 to a *closed* multicurve $\epsilon(\gamma)$ carried by T_0 by connecting any endpoints of γ at terminals of T_1 by the dotted arcs in the figure. For closed curves ϵ does not modify the multicurve, and the resulting weights on T_0 will be the sum of the upper

and lower case weights of T_1 : $p' = p + P, q' = q + Q, r' = r + R$. If γ consists of arcs where the weight of each terminal is 1, then the weights of the closed multicurve $\epsilon(\gamma)$ carried by T_0 will be $p' = p + P + 2, q' = q + Q + 2, r' = r + R + 2$. The +2s count the extensions and are indicated by dotted lines in Figure 13(b).

The involution π will preserve a multicurve carried by T_1 if and only if the curve's weights are preserved by π , that is $p = P, q = Q, r = R$, and terminals of equal weight are exchanged.

Lemma 11. *The involution π preserves no closed connected curve γ carried by T_1 .*

Proof. If γ is preserved by π , then its weights must be preserved by π , hence $p = P, q = Q, r = R$. Then $\epsilon(\gamma)$ is carried by T_0 and has even weights, each a sum of an equal lowercase and uppercase weight. The curves γ and μ then have intersection pattern $(2p, 2q)$. Since $2p$ and $2q$ are not relatively prime and μ is connected, the curve γ cannot be connected; see the discussion of intersection patterns in Section 3.1. \square

Lemma 12. *Let γ be a closed curve carried by T_1 . Then $\epsilon(\gamma)$ and $\epsilon(\pi(\gamma))$ have the same weights (and hence are isotopic) in T_0 .*

Proof. The involution changes the case of each of the weights of γ , then ϵ sums each lower and upper case weight. Thus the curves $\epsilon(\gamma)$ and $\epsilon(\pi(\gamma))$ have equal weights and are hence isotopic in T_0 . \square

When $p = P, q = Q, r = R$, then the involution π fixes the weight vector \vec{w} as well as the track T_1 , and we will say that $\{T_1 | \vec{w}\}$ is *invariant under π* . Recall that a weighted train track is really a shorthand for a multicurve drawn in a small neighborhood of the track. The weight component for each branch specifies the number of times the multicurve travels along that branch. If $\{T_1 | \vec{w}\}$ is invariant under π , then we will assume that the multicurve has been drawn carefully in $N(T_1)$ so that it is fixed setwise by π . We will say that $\{T_1 | \vec{w}\}$ contains two disjoint spirals if two disjoint spirals are formed in a neighborhood of T_1 by the multicurve prescribed by \vec{w} and some basis arc for a branch of T_1 .

Proposition 13. *Suppose that the weighted train track $\{T_1 | \vec{w}\}$ is invariant under π and contains a spiral. Then $\{T_1 | \vec{w}\}$ contains two disjoint spirals.*

This result is based on analyzing the rectangle cut out by the spiral, see Figure 4, and how the rectangle meets its image under the involution π . In particular, if the rectangle is not disjoint from its image under π , then we produce a fixed curve, contradicting earlier lemmas. It will follow that these two rectangles, and their corresponding spirals, are disjoint.

Proof. Recall that, since the weighted train track $\{T_1 | \vec{w}\}$ is invariant under π , we have constructed the following objects, each of which is fixed setwise but contains no fixed point under the action of π : a) a neighborhood $N(T_1)$ of T_1 , b) a collection of disjoint basis arcs, one for each branch, and c) the multicurve prescribed by \vec{w} .

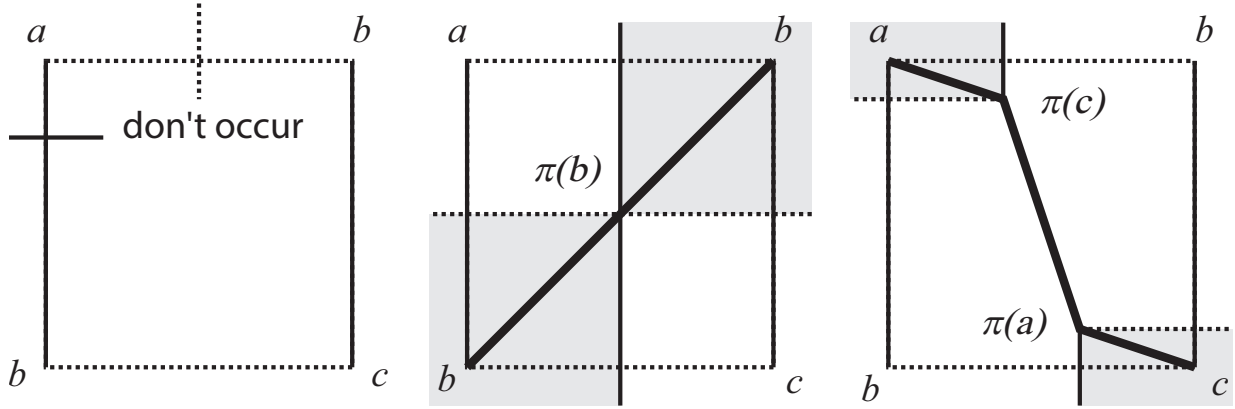


Figure 14: Intersections between R and $\pi(R)$. The vertical arcs are basis arcs (β), the horizontal arcs are portions of the multicurve (γ). The shaded region indicates $\pi(R)$.

Suppose that $\{T_1|\vec{w}\}$ does contain a spiral. Then γ , a subarc of the multicurve prescribed by \vec{w} , and β , a subarc of a basis arc, bound a rectangle R that meets itself in a single point as in Figure 4. Without loss of generality, we may assume that the rectangle R is oriented as in Figure 14; namely that b , the point of self-contact, occurs at the upper-right and lower-left corners of R , and a and c are the top-left and bottom-right corners of R , respectively. The top and bottom sides of the rectangle are subarcs of γ that connect at b and the left and right sides are subarcs of the basis arc β that also connect at b . Note that the entire drawing is reduced in T_1 , because no component of the multicurve can form a bigon with a basis arc.

We now consider the possible patterns of intersection $R \cap \pi(R)$ with the aim of showing that it is empty, see Figure 14. Since the involution π exchanges R and $\pi(R)$, the pattern of intersection appears precisely the same in each rectangle. The rectangle R will be cut across vertically by some subarcs of basis arcs, and horizontally by some subarcs of the multicurve specified by the weight vector. We can measure the *length* of a subarc of the multicurve or basis arc to be the number of intersections it has with the basis arcs or multicurve, respectively. Since the drawing is reduced, the lengths of the left and the right side of R are the same, and thus we can define the *height* of the rectangle R as the length of its left side. Similarly we can define the *width* of R as the length of its bottom side. Since π preserves both the collection of basis arcs and the multicurve, this pattern appears precisely the same in $\pi(R)$, and π can be regarded as an isometry, as it preserves the length of any arc. We study the intersection $R \cap \pi(R)$ through a sequence of claims, and ultimately conclude that the intersection is empty.

Claim. $\beta \cap \pi(\beta) = \emptyset$.

Under the action of π , every basis arc of the track is moved to a disjoint basis arc. The arc β is a subarc of a basis arc so the claim follows.

Claim. $\gamma \cap \pi(\gamma) = \emptyset$.

Let γ' be the component of the multicurve prescribed by \vec{w} and containing γ . If γ' is a closed curve, then $\gamma' \cap \pi(\gamma') = \emptyset$ by Lemma 11. If γ' is a simple arc, then $\gamma' \cap \pi(\gamma') = \emptyset$ by Corollary 10.

Claim. $R \cap \pi(R)$ is the union of rectangles, each containing, in opposite corners, a corner of R and a corner of $\pi(R)$.

Since π preserves both the set of basis arcs and the multicurve, the overlap consists of a union of rectangles that are bounded by boundary arcs of R and $\pi(R)$. In each component subrectangle, either the top is a subarc of R and the bottom a subarc of $\pi(R)$, or vice-versa, because the alternative would imply that the height of R is less than the height of $\pi(R)$, or vice-versa. Similarly, the left side is from R and right side from $\pi(R)$, or vice-versa. It follows that every subrectangle contains both a corner of R and a corner of $\pi(R)$.

Claim. $\pi(b) \notin R$.

Suppose that $\pi(b) \in R$. By prior claims $\pi(\gamma)$ and $\pi(\beta)$ cut R into quadrants and $R \cap \pi(R)$ includes either the two quadrants containing a and c or the two quadrants containing b . Since π is an orientation-preserving map on the torus, the point $\pi(b)$ is both a bottom left and a top right vertex of a quadrant in $R \cap \pi(R)$, hence these two quadrants must contain the b corners of R . See Figure 14, middle picture. Now, π must exchange these quadrants, for otherwise it would send one to itself and this would imply that π has a fixed point in that quadrant, by the Brouwer's fixed-point theorem for a disk. In one quadrant choose a diagonal joining b to $\pi(b)$. Then π applied to that diagonal is a diagonal in the other quadrant joining $\pi(b)$ to b , and the union of the diagonal and its image is a closed connected curve that is carried by T_1 and is invariant under π . This contradicts Lemma 11.

Claim. $\pi(a) \notin R$ and $\pi(c) \notin R$.

Suppose $\pi(a) \in R$. Then the $\pi(a)$ corner of $\pi(R)$ overlaps a corner of R . It cannot overlap a b corner, for this would imply that $\pi(b) \in R$, contradicting the previous claim. Nor can it overlap the a corner. For in this case we would see a rectangle of intersection between the top-left corners of R and $\pi(R)$. But such a rectangle of intersection would be invariant under π , and would contain a fixed point. So we consider what happens if the $\pi(a)$ corner of $\pi(R)$ overlaps the c corner of R . Because the intersection pattern is symmetric, we also see the $\pi(c)$ corner of $\pi(R)$ overlapping the a corner of R . In R choose two connecting arcs, one from a to $\pi(c)$ and the other from $\pi(c)$ to $\pi(a)$, see rightmost image in Figure 14. Then π applied to this pair of connecting arcs is another pair of connecting arcs in $\pi(R)$, the first from $\pi(a)$ to c and the other from c to a (not pictured). The union of the four arcs is a closed connected curve that is carried by T_1 and invariant under π , again in contradiction to Lemma 11. The same argument proves $\pi(c) \notin R$.

Since an overlap would imply that a corner of $\pi(R)$ is contained in R , and this does not occur, we conclude that the rectangles R and $\pi(R)$ are disjoint. A slight neighborhood of R is a spiral annulus A that is disjoint from the spiral annulus $\pi(A)$. This proves the proposition. \square

Theorem 14. *The weighted track $\{T_1|p = P = F_n - 1, q = Q = F_{n-1} - 1, r = R = F_{n-2} - 1, \text{ terminals have weight } 1\}$ contains no d -spiral for $d \geq 1$.*

Proof. If there is a d -spiral with $d \geq 1$, then there is a 1-spiral, and Proposition 13 implies that we can actually find two disjoint 1-spirals. By Lemma 12, ϵ maps these to a pair of disjoint parallel spirals in $\{T_0|p' = 2F_n, q = 2F_{n-1}, r = 2F_{n-2}\}$.

But then, Lemma 3 implies that β , a basis arc, and α , a component of the multicurve prescribed by the weights, form a 2-spiral in $\{T_0|p' = 2F_n, q' = 2F_{n-1}, r' = 2F_{n-2}\}$. (Note that Lemma 3 does not require that α and α' are subarcs of the same multicurve, only that the two spirals are disjoint, which forces α through the α' spiral and vice-versa.)

Now the multicurve $\{T_0|p' = 2F_n, q' = 2F_{n-1}, r' = 2F_{n-2}\}$ has two components, each with equal weights. Hence α is described by the weighted track $\{T_0|p' = F_n, q' = F_{n-1}, r' = F_{n-2}\}$. But this is in direct contradiction to Corollary 8 which states, in particular, that this weighted track contains no 2-spiral. \square

4 Avoiding Spirals in the Plane

In Section 4.1 we construct a spiral-free drawing of two (reduced) curves in the plane with an arbitrarily large number of intersection points. This allows us to give, in Section 4.2, a counterexample to a proof by Pach and Tóth [8] that the number of intersections in a minimal realization of a string graph is at most exponential.

4.1 Spiral-Free Curves in the Plane

We are now ready to prove our ultimate goal, that the planar weighted track $\{T_2|p = F_n - 1, q = F_{n-1} - 1, r = F_{n-2} - 1, \text{ terminals have weight } 1\}$, pictured in Figure 15, is spiral-free. Our proof exploits the fact that the weighted track T_1 is a *double covering* of the weighted T_2 track. If the weighted T_2 track contains a spiral, we will demonstrate that it can be either be *lifted* (pulled back) to T_1 , which contradicts Proposition 13, or that the weighted track T_1 contains a fixed curve, which contradicts Lemma 11.

There is a strong similarity between the (weighted) tracks T_1 and T_2 , a similarity induced by π . We can view T_1 as formed by cutting each of the loops of T_2 , taking two copies, and then gluing them together. Or, alternatively we can see that T_2 is a quotient of T_1 under the action of π . Let $N(T_1)$ be a regular neighborhood of T_1 that is invariant under the action of π , but for which no point is fixed by π . Let $N(T_2)$ be the *quotient space* $N(T_1)/(x \sim \pi(x))$, where each each point has been identified with its image under π . Then, there is a natural projection $\rho : N(T_1) \rightarrow N(T_2)$ sending each point in $N(T_1)$ to its corresponding identified point: $\rho(x) = \rho(\pi(x))$. In fact, ρ is a *local homeomorphism*, and restricts to a homeomorphism of any neighborhood $U \subset N(T_1)$ that is disjoint from $\pi(U) \subset N(T_1)$. Together, the space $N(T_1)$ and the map ρ are referred to as a *covering space* of $N(T_2)$; see [6, Chapter 1.3]. Covering spaces have very strong properties. Here we will use only the fact that any simply-connected region $U \subset N(T_2)$ *lifts to* $N(T_1)$, that is, the inverse image $\rho^{-1}(U)$ consists of n disjoint regions $\{U_1, U_2, \dots, U_n\} \subset N(T_1)$,

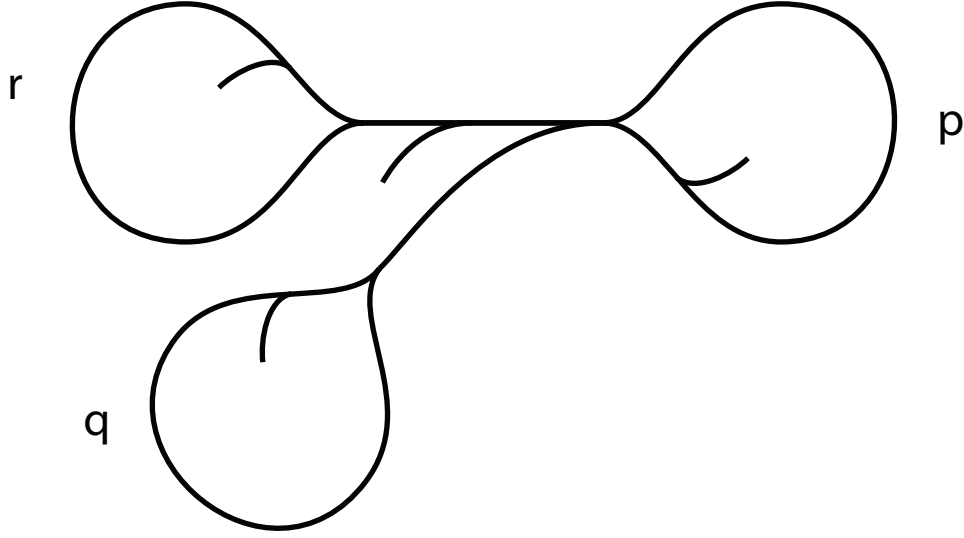


Figure 15: The track T_2 . The weighted track $\{T_2|p = F_n - 1, q = F_{n-1} - 1, r = F_{n-2} - 1, \text{terminals have weight } 1\}$ has no spirals.

each homeomorphic to U . In our case, $N(T_1)$ is a double-cover of $N(T_2)$, that is, $n = 2$. Points, arcs, disks and embedded rectangles are all simply connected, so each will lift to two disjoint copies in $N(T_1)$.

Because the lower case and upper case weights are equal, ρ can also be regarded as a map between the weighted tracks $\rho : \{T_1|p = P = F_n - 1, q = Q = F_{n-1} - 1, r = R = F_{n-2} - 1, \text{terminals have weight } 1\} \rightarrow \{T_2|p = F_n - 1, q = F_{n-1} - 1, r = F_{n-2} - 1, \text{terminals have weight } 1\}$ that converts to lower case and projects induced curves onto induced curves. In fact, though we will not prove it here, the multicurve specified by these weights in $N(T_2)$ is a union of two properly embedded arcs (contains no closed curves), and therefore lifts to the union of precisely four properly embedded arcs in $N(T_1)$.

There is one essential difference between T_1 and T_2 : T_2 is planar whereas T_1 can only embed in surfaces of genus at least 1.

Theorem 15. *The weighted train track $\{T_2|p = F_n - 1, q = F_{n-1} - 1, r = F_{n-2} - 1, \text{terminals have weight } 1\}$ contains no spiral.*

Proof. By way of contradiction, assume there is a spiral, thus there is a rectangle with a single point of intersection b formed by the induced multicurve and a basis arc in the neighborhood of T_2 . We cannot lift this rectangle since the point of self-contact prevents it from being simply connected. In an abuse of notation we will let R denote the rectangle with only the point b removed, that is, a rectangle with two open corners. This R is simply connected and therefore lifts to two “rectangles”, R_1 and R_2 in the double cover, a neighborhood of the weighted track $\{T_1|p = P = F_n - 1, q = Q = F_{n-1} - 1, r = R = F_{n-2} - 1, \text{terminals have weight } 1\}$. There are also two lifts of b : b_1 and b_2 . There are two possibilities: 1) each of the rectangles R_1 and R_2 uses only one of the points b_1 and b_2 , or

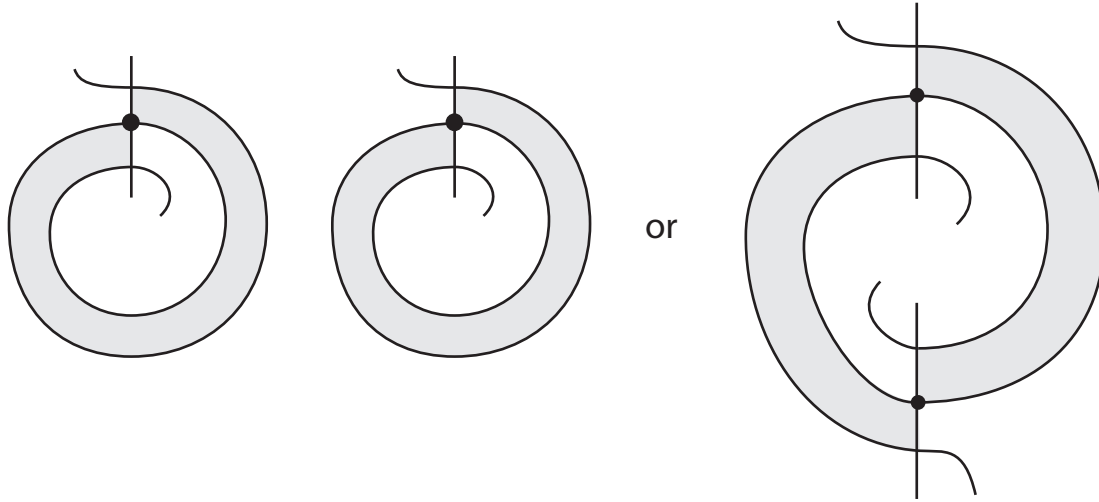


Figure 16: The rectangles in $N(T_1)$ can either each have their own b or they share the two b 's.

2) R_1 and R_2 are chained together, each using both b_1 and b_2 . See Figure 16. In the former case, R_1 and R_2 are both spirals, and either one can be used to contradict Theorem 14.

The latter case can also be seen to be a contradiction. While the involution π exchanges R_1 and R_2 , it preserves the union $R_1 \cup R_2 \cup b_1 \cup b_2$. Let β_1 be the diagonal arc of R_1 connecting b_1 and b_2 , and $\beta_2 = \pi(\beta_1)$ the diagonal of R_2 . But then π preserves the closed curve $\beta = \beta_1 \cup \beta_2$, contradicting Lemma 11. \square

4.2 A Counterexample to Pach and Tóth

Pach and Tóth [8] proved that for every $n \geq 1$, every pair of curves in the plane with reduced intersection and with sufficiently many intersections, forms either a spiral of depth n or a fold of width n . Their paper claims to show that in a minimal realization of a string graph both the depth of a spiral and the width of a fold are bounded above in the number of curves. An upper bound on the number of intersections between each pair of curves, hence of the entire string graph realization would follow. Their argument against spirals is correct: sufficiently deep spirals can be used to reduce the number of intersections in a realization, contradicting the minimality of the realization.

However, their argument that the existence of a wide fold implies the existence of a deep spiral is unfortunately incorrect and cannot be fixed easily.

The main idea in the proof is to start with the original wide fold, and assuming there are no deep spirals, construct a sequence of “iterated” folds of smaller widths, and in each iteration find an obstruction that prevents easy simplification of the drawing. The obstruction in each iteration is a pair (g, v) where g is an edge “cutting all the way through” the fold and terminating in a vertex v inside the fold; see Figure 17. It is then argued that for each iteration a new obstruction is needed which would imply that after at most $2m + 1$

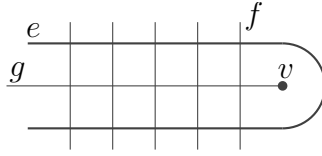


Figure 17: A curve g cutting all the way through a fold formed by e and f . In [8], this is referred to as an empty path of type 2.

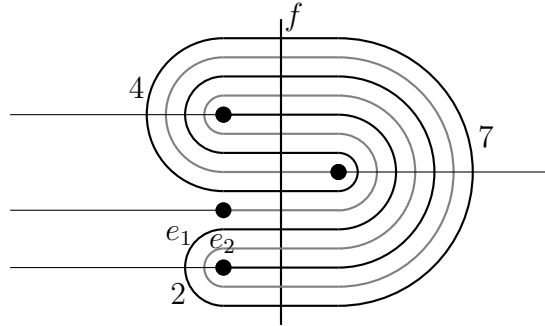


Figure 18: A system of curves carried by the train track T_2 on Fig. 15 for $n = 6$, extended to a drawing of a graph with 7 edges.

iterations the drawing can be simplified. This claim, however, is false. We construct a counterexample containing a pair of curves forming an arbitrarily wide fold and having no spirals or bigons, with only four possible pairs (g, v) that can serve as obstructions.

The counterexample consists of two edges e_1, e_2 that are carried by the train track T_2 in Figure 15, and an edge f that crosses the train track transversely in the central part. We also add four auxiliary edges joined to the endpoints of e_1 and e_2 . See Figure 18 for the case $n = 6$.

By Theorem 15 the curves e_1 and f do not form a spiral. Therefore, they form an arbitrarily wide fold if n is arbitrarily large (see [8], also [10]). However, only the pairs (v, e_i) where v is an endpoint of e_i are available as obstructions to simplifying the folds, so the number of obstructions is fixed and does not increase with the number of intersections.

This gap in Pach and Tóth's argument cannot be filled easily. In their argument, folds are simplified only by local redrawings of the pairs of curves g, h that form an empty bigon, or a bigon which may contain some vertices but all edges that cross the part of the boundary formed by g also cross the opposite part of the boundary formed by h . In our example, no such bigons exist, and there are no spirals, so none of their redrawing techniques apply.

It is possible to simplify the drawing in our example by a simultaneous local redrawing of both edges e_1 and e_2 . However, it is not clear how to generalize this operation for systems of more than two curves. The related *Simple shortcut problem*, introduced by

Štefankovič [15, Section 4.2], asks about the possibility of simplifying a drawing of a graph in the neighborhood of one edge, and it is still wide open.

References

- [1] B. Alspach, P. Hell and D. J. Miller (editors), *Algorithmic aspects of combinatorics*, North-Holland Publishing Co., Amsterdam (1978), Conference held at the Qualicum College Inn, Vancouver Island, B.C., May 17–21, 1976, *Annals of Discrete Math.* **2** (1978).
- [2] S. Benzer, On the topology of the genetic fine structure, *Proceedings of the National Academy of Science* **45** (1959), 1607–1620.
- [3] É. Colin de Verdière, Computational topology of graphs on surfaces, *Handbook of discrete and computational geometry*, edited by J. E. Goodman, J. O’Rourke and C. D. Tóth, Discrete Mathematics and its Applications (Boca Raton), CRC Press, Boca Raton, FL, ISBN 978-1-4987-1139-5 (2018) xxi+1927, third edition.
- [4] B. Farb and D. Margalit, *A primer on mapping class groups*, vol. 49 of *Princeton Mathematical Series*, Princeton University Press, Princeton, NJ (2012), ISBN 978-0-691-14794-9.
- [5] R. L. Graham, Problem 1, *Open Problems at 5th Hungarian Colloquium on Combinatorics* (1976) .
- [6] A. Hatcher, *Algebraic topology*, Cambridge University Press, Cambridge (2002), ISBN 0-521-79160-X; 0-521-79540-0.
- [7] J. Kratochvíl and J. Matoušek, String graphs requiring exponential representations, *J. Combin. Theory Ser. B* **53**(1) (1991), 1–4.
- [8] J. Pach and G. Tóth, Recognizing string graphs is decidable, *Discrete Comput. Geom.* **28**(4) (2002), 593–606, Discrete and computational geometry and graph drawing (Columbia, SC, 2001).
- [9] R. C. Penner and J. L. Harer, *Combinatorics of train tracks*, vol. 125 of *Annals of Mathematics Studies*, Princeton University Press, Princeton, NJ (1992), ISBN 0-691-08764-4; 0-691-02531-2.
- [10] M. Schaefer, E. Sedgwick and D. Štefankovič, Spiraling and folding: The word view, *Algorithmica* **60**(3) (2011), 609–626.
- [11] M. Schaefer, E. Sedgwick and D. Štefankovič, Recognizing string graphs in NP, *J. Comput. System Sci.* **67**(2) (2003), 365–380, special issue on STOC2002 (Montreal, QC).

- [12] M. Schaefer, E. Sedgwick and D. Štefankovič, Spiralling and folding: The topological view, *Proceedings of the 19th Annual Canadian Conference on Computational Geometry, CCCG 2007, August 20-22, 2007, Carleton University, Ottawa, Canada*, edited by P. Bose (2007) 73–76.
- [13] M. Schaefer and D. Štefankovič, Decidability of string graphs, *J. Comput. System Sci.* **68**(2) (2004), 319–334.
- [14] F. W. Sinden, Topology of thin film circuits, *Bell System Technical Journal* **45** (1966), 1639–1662.
- [15] D. Štefankovič, *Algorithms for simple curves on surfaces, string graphs, and crossing numbers*, Ph.D. thesis, University of Chicago, Chicago, IL, USA (2005).
- [16] J. Stillwell, *Classical topology and combinatorial group theory*, vol. 72 of *Graduate Texts in Mathematics*, second ed., Springer-Verlag, New York (1993), ISBN 0-387-97970-0.